NASA TECHNICAL NOTE

NASA TN D-7709

NASA TN D-7709

HIGH-EFFICIENCY, 200-WATT, 12-GIGAHERTZ TRAVELING WAVE TUBE

by Henry G. Kosmahl, B. D. McNary, and Otto Sauseng

Lewis Research Center

Cleveland, Ohio 44135

NATIONAL AERONAUTICS AND SPACE ADMINISTRATION • WASHINGTON, D. C. • JUNE 1974

1. Report No.	2. Government Accession No.	3. Recipient's Catalog No.
NASA TN D-7709		

4. Title and Subtitle	5. Report Date
HIGH-EFFICIENCY, 200-WATT, 12-GIGAHERTZ TRAVELING WAVE TUBE	June 1974
	6. Performing Organization Code

7. Author(s)	8. Performing Organization Report No.
Henry G. Kosmahl, Lewis Research Center, B. D. McNary, and Otto Sauseng, Litton Industries, San Carlos, California	E-7910
	10. Work Unit No. 502-23

9. Performing Organization Name and Address	11. Contract or Grant No.
Lewis Research Center National Aeronautics and Space Administration Cleveland, Ohio 44135	
	13. Type of Report and Period Covered

12. Sponsoring Agency Name and Address	14. Sponsoring Agency Code
National Aeronautics and Space Administration Washington, D.C. 20546	

15. Supplementary Notes

16. Abstract

Design and performance of a highly efficient experimental 200-watt traveling wave tube for space communications are described. The tube uses a coupled cavity slow wave structure with periodic permanent magnet focusing. A two-step velocity taper is incorporated in the slow wave structure for velocity resynchronization with the modulated beam. The spent beam is reconditioned in a refocusing section before it is collected in a novel multistage depressed collector. The collector is radiation cooled and heat insulated from the tube body. At saturation the tube provides peak output power of 240 watts with a 35-dB gain and an overall maximum efficiency of 56 percent.

17. Key Words (Suggested by Author(s))	18. Distribution Statement
Traveling wave tube High efficiency Space communications	Unclassified - unlimited Category 09

19. Security Classif. (of this report)	20. Security Classif. (of this page)	21. No. of Pages	22. Price*
Unclassified	Unclassified	18	$3.00

* For sale by the National Technical Information Service, Springfield, Virginia 22151

HIGH-EFFICIENCY, 200-WATT, 12-GIGAHERTZ TRAVELING WAVE TUBE*

by Henry G. Kosmahl, B. D. McNary,† and Otto Sauseng**

Lewis Research Center

SUMMARY

Design and performance of a highly efficient experimental 200-watt traveling wave tube for space communications are described. The tube uses a coupled cavity slow wave structure with periodic permanent magnet focusing. A two-step velocity taper is incorporated in the slow wave structure for velocity resynchronization with the modulated beam. The spent beam is reconditioned in a refocusing section before it is collected in a novel multistage depressed collector. The collector is radiation cooled and heat insulated from the tube body. At saturation the tube provides a peak output power of 240 watts with a 35-dB gain and an overall maximum efficiency of 56 percent.

INTRODUCTION

The tube to be described here is intended for use in an advanced high power satellite communication system (Communication Technology Satellite). For the use of high power tubes in communication satellite systems it is highly desirable to achieve:

(1) Overall efficiency of more than 50 percent

(2) High reliability with a tube-life of at least 2 years

(3) Radiation cooling into space environment

(4) Compliance with strict communication performance requirements

(5) Survival of the tubes during the severe vibrations of the launching operation.

These are rather high performance requirements for a 200-watt tube at 12 gigahertz, especially with respect to efficiency. The tube design incorporates, therefore, several

*Presented in part at the IEEE International Electron Devices Meeting, December 5, 1973.

†Litton Industries, San Carlos, California.

**Litton Industries, San Carlos, California; now at Hughes Aircraft Co., Torrance, California.

advanced features, including a novel radiation cooled multistage collector configuration developed at NASA Lewis Research Center (refs. 1 and 2). This collector makes possible an overall efficiency of more than 50 percent in spite of relatively large circuit and interception losses. Heat transfer to the space environment is thereby accomplished at moderate temperatures.

SYMBOLS

a	tunnel radius
B	magnetic induction
BW	bandwidth
b	Pierce velocity parameter, $(u_o - v_p)/v_p C$
C	Pierce gain parameter $(K/4R_o)^{1/3}$
d	Pierce attenuation parameter
f	frequency
h	cavity height
I_c	collector electrode current
I_o	dc cathode current
K	interaction impedance
L	loss on circuit, dB
$2l_c$	magnetic focusing period
P	power
Q	quality factor of cavities
QC	Pierce's space charge parameter
R_o	beam impedance, V_o/I_o
R_s	shunt resistance of cavities
u_o	dc electron velocity
V	potential, V
V_o	cathode to body voltage
v_g	group velocity
v_p	phase velocity
γ	radial propagation constant

η	efficiency
λ_p	plasma wavelength
Φ	phase shift angle per cavity, radians
$\dot{\varphi}$	angular velocity, radians/sec
ω	$2\pi f$

Subscripts:

c	collector
ct	circuit
dis	dissipation
in	input
n	collector electrode number
o	standard section of TWT
out	output
rec	recovered
rf	radiofrequency
T	tapered section of TWT
TWT	traveling wave tube

CHOICE OF SLOW WAVE STRUCTURE

The coupled cavity slow wave structure was selected over a helix-type slow wave circuit because its all-metal structure provides better heat transfer and thermal capacity with lower temperatures. This choice is especially important above 200 watts because it is expected to result in higher tube reliability and longer tube life.

THERMAL AND MECHANICAL DESIGN

Figure 1(a) shows an experimental version of the tube with its support structure, and figure 1(b) shows the cross section through the tube. The tube is mounted on the spacecraft in such a way that the collector protrudes outside the spacecraft envelope so that it can radiate directly into space. The collector envelope is comparatively large so that the radiation temperature of the collector surface is kept within moderate limits

(less than 200° C with a measured heat dissipation of 90 W at saturation). Heat transfer from the collector electrodes to the collector envelope is also by radiation. Local hot spots on the collector electrodes are estimated to be less than 400° C. The collector is thermally insulated from the tube body by a heat choke. The waste heat from the tube body is disposed of by a radiation panel (base plate) on which the tube is mounted. Heat to the panel is transferred by conduction from the slow wave circuit. The split ring magnets are separated to provide room for two massive axial conduction rails along the sides of the circuit. The waste heat from the tube body was measured to be 115 watts. One fourth of this heat was caused by 6 percent beam interception. The cathode heater produces 6 watts dissipation. The rest was generated by radiofrequency (rf) losses of the slow wave circuit. Without rf drive the beam interception was 2 percent, and the body heat loss was 22 watts, including heater power.

Total weight of the tube including housing structure, waveguide connections, and sensors is less than 13 kilograms.

ELECTRONIC DESIGN

Figure 2 shows a schematic of the velocity profile of the circuit and it includes a list of the tube parameters at 12.06 gigahertz, based on cold test data. The tube circuit is separated into three gain sections by two internal severs to ensure tube stability. No other tube stabilization techniques are used, such as loss buttons or distributed loss. The output section incorporates a two-step velocity taper for efficiency enhancement. The tube is operated in "undervoltaged" condition (velocity parameter $b = 0$) in order to assure good beam bunching for velocity resynchronization.

The length of the output gain section (prior to the velocity taper) has been chosen large enough to avoid efficiency degradations due to sever effects. The estimated small signal gain in this section is 23 dB. The velocity taper was designed with the aid of a large signal computer program using circuit parameters based on cold test data. The analysis takes the reduction of the interaction impedance in the taper into account, as well as the increase of the losses in the taper. Empirically the interaction impedance K_T in the taper was found to be reduced proportional to the square of the phase-velocity reduction (period reduction) (ref. 3). The losses L_T in the taper section were found to increase inversely with impedance. The predicted electronic efficiency was 34 percent at 12 gigahertz, compared to 30 percent measured. Without velocity taper the electronic efficiency would have been on the order of 15 percent. The rf circuit losses are predicted to cause a reduction of the electronic efficiency to 70 percent of the efficiency obtainable with a lossless circuit.

BANDWIDTH AND CIRCUIT LOSSES

The coupled cavity circuit has bandpass filter characteristics with a bandwidth determined primarily by the width of the coupling slot. For amplification the electron beam is synchronized with the first forward wave space harmonic. Ideally both the interaction impedance and the losses should be inversely proportional to the cold bandwidth. It is generally desirable to design the cold bandwidth as small as possible to achieve a high interaction impedance. Coupled cavity tubes can however only utilize a fraction of the cold bandwidth for amplification because of the dispersion of the circuit. It is therefore necessary to design for a much larger cold bandwidth than the operational bandwidth. For conventional tubes it has become practice to provide a cold bandwidth about four times as large as the operating bandwidth. Cold tests with such a circuit revealed, however, that an even larger cold bandwidth was required to obtain acceptably small losses.

Figure 3 shows the predicted efficiency reduction due to circuit losses. For the initially observed losses on the order of 0.3 to 0.4 dB per cavity the efficiency would be reduced by a factor of more than two. The circuit design was therefore reviewed and the design of larger cold bandwidths was explored, since the circuit losses are expected to become smaller with larger cold bandwidths. At the same time, the cavity and coupling slot configuration were modified with the objective of lowering the circuit losses. A thin coupling slot was used similar to that described in the Varian report (ref. 4). In addition the slot edges and the ferrule base were rounded off. In order to obtain losses of less than 0.1 dB per cavity, it was found necessary to increase the cold bandwidth to 1300 megahertz.

Figure 4 shows that the circuit losses can be reduced to sufficiently small values of 0.07 to 0.11 dB per cavity in the untapered section of the tube when the slot width W and the cold bandwidth are adequately increased. The loss reduction is found to be more rapid with bandwidth than would be expected from the conventional circuit loss theory (ref. 5). This theory predicts loss increases at the band center to be inversely proportional to the group velocity and to the cold bandwidth.

Unfortunately it is not possible to maintain the relative low loss per cavity through the tapered section of the traveling wave tube (TWT). It is known that both the group velocity v_g and the height of the cavity h are reduced in tapered sections compared to standard cavities. We know also that losses are proportional to $1/(v_g Q)$ or $1/(v_g h)$ with the result that the losses in the output tapered section are approximately doubled. Since the power lost is proportional to the square of the voltage across the gap and the voltages are highest in the tapered (saturated) region, approximately 70 percent of all skin losses takes place in the last 10 cavities of the TWT. A fairly accurate determination of this loss is easily obtained from measuring the total heat dissipation (exclusive of collector) in the TWT body. This heat consists of heater power plus interception power plus skin

loss power. The interception power at zero drive is easily measured. The power intercepted due to rf defocusing can be estimated to be not smaller than the power carried by the slowest electrons in the stream (from computer output). In the TWT of this report the low energy electrons had approximately 0.4 of the dc energy. The minimum value of interception power was determined to be 27 watts. With the heater power of 6 watts and the total body power being 115±10 watts, the skin effect loss is 107±10 watts. This gives a circuit efficiency of $237/(237 + 82) = 0.74$, which is a significant reduction. In view of this fact the usefulness of the last few heavily tapered cavities, which contribute to about one half of the skin losses and add only little to the rf power, is dubious.

The group velocity is proportional to the slope $df/d\Phi$ and therefore to the bandwidth. The operating band is centered at a rather small phase angle for the low loss circuit, while a conventional bandwidth design would normally be centered around $\Phi = 1.4\,\pi$ phase angle. This smaller phase angle was chosen for the low loss circuit in order to obtain a higher interaction impedance. The interaction impedance of a slow wave structure is known to decrease inversely proportional with the group velocity and, at bandcenter, it decreases inversely with the cold bandwidth. The improvement of the interaction impedance at lower frequencies (and smaller phase angles) is illustrated with the measured data of figure 5. Even though the interaction impedance in the operating range is lower than that of a conventional bandwidth design, a careful taper design makes it still possible to achieve good electronic efficiencies on the order of 30 percent. Figure 6 illustrates the bandwidth characteristics with this circuit. These data show power output with constant drive over a frequency range. Flat response can be achieved over a range of about 170 megahertz, or about twice the specified hot bandwidth.

GUN AND FOCUSING DESIGN

The gun is of the conventional Pierce type, with an insulated anode to protect the cathode against ion bombardment. For this purpose a positive voltage of several hundred volts is applied to the anode. Cathode material is tungsten matrix with a cathode loading of 450 mA/cm^2. This cathode material is known to be rugged in operation and is expected to provide long tube life. The gun is completely magnetically shielded. The magnetic focusing design with half ring magnets extends over two cavity periods. This double period configuration is commonly used in PPM focused coupled cavity tubes and achieves higher peak fields with smaller transverse perturbation fields due to the coupling slots than single-period focusing. The focusing stability is generally assumed to be equal to that of single-period focusing. For this design the focusing stability $\lambda_p/2l_c = 6.1$ is high. Magnet material is Samarium Cobalt, and the required peak field

is on the order of 1500 gauss. Beam transmission into the collector is 98 percent without rf and 94 percent at saturation.

REFOCUSING SECTION

Before the spent electron beam enters the multistage collector, it is reconditioned in a refocusing section. The refocusing section was originated and designed at NASA Lewis Research Center (ref. 6) and is essential for the highly efficient operation of multistage collectors.

A schematic of the refocusing section is shown in figure 7. In the refocusing section the magnetic focusing field is gradually reduced over a significant length, such that the corresponding beam expansion can be considered adiabatic. The field decay is followed by a short plateau field which is terminated at the entrance plane of the collector. The refocusing section has two important functions:

(1) Beam expansion - The spent beam is allowed to expand so that its space charge forces become small. This will reduce faulty velocity sorting in the multistage collector due to space charge effects.

(2) Refocusing - The expanded spent beam is refocused such that it enters the collector essentially with parallel trajectories. Properly arranged adiabatic expansion of the beam reduces radial velocity components of the spent beam and thus makes the velocity sorting of the collector more effective. The shape of the refocusing field and of a typical refocused trajectory are shown in figure 7. The physics of spent beam refocusing can be qualitatively shown with the use of the following three electronoptical relations:

(a) Busch's theorem:

$$\dot{\varphi} = \frac{e}{2m} B_z$$

(b) Adiabatic beam expansion:

$$\frac{r_1}{r_0} = \frac{B_{z0}}{B_{z1}}$$

(c) Invariance of electron dipole moment:

$$(\dot{r}^2 + r^2\dot{\varphi}^2)^{1/2} r^2 = \text{constant}$$

The radial velocity reduction is as follows:

$$\dot{r}_1^2 = \dot{r}_0^2\left(\frac{B_{z1}}{B_{z0}}\right)^4 - r_0^2\dot{\varphi}_0^2\left[1 - \left(\frac{B_{z1}}{B_{z0}}\right)^4\right]$$

where $\ddot{r} = 0$ and $B_c = 0$.

The design of the refocusing section was studied in great detail at NASA Lewis Research Center (ref. 7) and at General Electric Co. for Klystrons (ref. 8). It was found that the magnitude of the plateau field is also critical with respect to the reduction of the radial rms velocities. The radial velocities can be reduced by nearly a factor of two and sometimes two and one-half with an optimum plateau-field design.

The refocusing field was implemented in the tube with permanent magnets. A field reversal between decay field and plateau field was incorporated in order to minimize magnetic leakage fields into the collector. Figure 8 shows the axial field distribution measured on this design.

MULTISTAGE COLLECTOR

The multistage collector is a key component in achieving high efficiency. Its basic concepts and functioning are described in reference 1. It consists of nine depressible collector electrodes as shown in the schematic of figure 9. The voltages and positions of the electrodes have been selected to achieve the following:

(1) Optimum efficiency enhancement at saturation - The voltages of the available number of collector electrodes have been selected to achieve maximum efficiency enhancement at saturation. This is determined by the kinetic energy distribution of the spent beam.

(2) Minimize lens effects of the electrodes - The position of the collector electrodes has been chosen to achieve essentially a uniform electrostatic deceleration field in the most negative collector region and a very weakly decelerating field in the vicinity of the injection hole. The length of the trajectories is much larger than the radius of the beam at injection which makes the beam appear as a point source.

Velocity sorting is achieved by radial deflection forces caused by the conical shape of the collector electrodes; the endspike at cathode potential provides additional radial deflection which acts mainly on the high energy electrons. Secondary emission is almost absent because of automatic suppression in negative fields. Figure 10 shows collector current distribution both at saturation and without rf drive. At saturation the collector efficiency is 82.5 percent, with an overall TWT efficiency of 56 percent. The total electric power requirement is then 424 watts, including heater power. Although the col-

lector was designed for optimum operation at saturation, it can be seen that it performs very well also with no rf drive, when most of the current is collected with the last two electrodes. The collector efficiency without rf was measured at 86.1 percent, with an overall power requirement of 122 watts. This demonstrates the excellent performance characteristics of the multistage collector over a wide range of operating conditions of the drive. Removing four of the less important electrodes would decrease the overall efficiency by only $1\frac{1}{2}$ percent. Were the collector the only source of losses in the tube, the overall efficiency would be in excess of 70 percent. The collector losses are approximately 80 watts at saturation. The body losses, composed of circuit losses, interception losses, and heater power were measured to be 115±10 watts. They represent the largest source of deficiency, almost one half of the useful power output.

The collector efficiency η_{coll} was computed from electrical and steady-state thermal measurements of heat dissipation in the tube body and the (thermally insulated) collector with carefully calibrated equipment at Lewis Research Center. The collector efficiency, defined as kinetic beam power recovered in the collector over total beam input power into the collector, was determined from two independent measurements:

$$\eta_{coll} = \frac{P_{rec}}{P_{rec} + P_{dis}}$$

$$\eta_{coll} = \frac{P_{rec}}{I_o V_o - P_{rf} - P_{TWT} + P_{heater}}$$

where $P_{rec} = \sum_n I_{cn} V_{cn}$, with I_{cn} and V_{cn} the current and voltage of the n^{th} collector electrode (to body), respectively; P_{dis} is the thermal power dissipated in the collector assembly, and P_{TWT} is the heat power dissipated in the TWT from interception, skin effect losses, and heater. The two formulas give agreement within 5 percentage points with the average being 82.5 percent at saturation. This result was achieved with the collector working on a beam having a substantial velocity spread, since approximately 50 percent of the beam power is used up in the tube. The accuracy of thermal measurements is ±10 watts. The aforementioned results present record efficiencies for the entire TWT and the multistage depressed collector (MDC) at any frequency.

CONCLUSIONS

An advanced design, coupled cavity traveling wave tube (TWT) has been developed which features several novel elements: a two-step velocity taper enhances the power

output efficiency by a factor of about two compared to an untapered design; a magnetic beam refocusing section acts upon the spent beam prior to injection into the multistage depressed collector (MDC) by expanding the beam and reducing its current density and by reducing by a factor of about two the rms values of the angles of the trajectories; and a novel multistage depressed collector returning approximately 80 percent of the received beam power back to the power supply. The overall maximum tube efficiency of 56 percent achieved at the design frequency of 12 gigahertz and the MDC efficiency of 81 percent represent record performance for the TWT and the MDC at any frequency.

The skin effect (circuit) losses which amount to more than 90 watts represent the major defficiency of the design. Together with the beam interception power of approximately 30 watts, these two losses prevent the achievement of overall efficiencies in excess of 75 percent. Since most of the circuit loss takes place in the last, heavily tapered cavities, the use of the "voltage jump" efficiency enhancement technique (as described in NASA CR-72450), which does not increase the loss per cavity, should be given a serious consideration.

Lewis Research Center,
National Aeronautics and Space Administration,
Cleveland, Ohio, March 29, 1974,
502-23.

REFERENCES

1. Kosmahl, Henry G.: A Novel Axisymmetric, Electrostatic Collector for Linear Beam Microwave Tubes. NASA TN D-6093, 1971.

2. Kosmahl, Henry G.: Electrostatic Collector for Charged Particles. U. S. Patent No. 3, 702, 951, 1972.

3. Sauseng, O. G.; Basiulis, A.; and Tammaru, I.: Analytical Study Program to Develop the Theoretical Design of Traveling-Wave Tubes. HAC-EDD-W-2646, Hughes Aircraft Co. (NASA CR-72450), 1968.

4. Ayers, W. R.; and Harman, W. A.: Design, Construction and Evaluation of a 12. 2 GHz, 4. 0 KW-CW Coupled-Cavity Traveling Wave Tube. Varian Associates (NASA CR-120920), 1973.

5. Pierce, John R.: Traveling-Wave Tubes. Van Nostrand Co., 1950, p. 95.

6. Kosmahl, Henry G.: An Electron Beam Controller. U. S. Patent No. 3, 764, 850, 1973.

7. Stankiewicz, N.: Evaluation of Magnetic Refocusing in Linear-Beam Microwave Tubes. NASA TN D-7660, 1974.

8. Branch, G. M.; and Neugebauer, W.: Refocusing of the Spent Axisymmetric Beam in Klystron Tubes. General Electric Co. (NASA CR-121114), 1972.

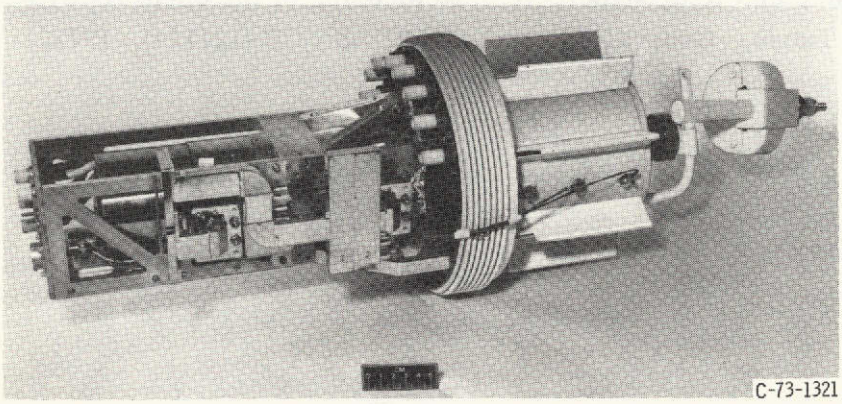

(a) Photograph of 12-gigahertz, 200-watt experimental tube with tube mount, heat choke, collector envelope with radiation fins, and VAC ion pump.

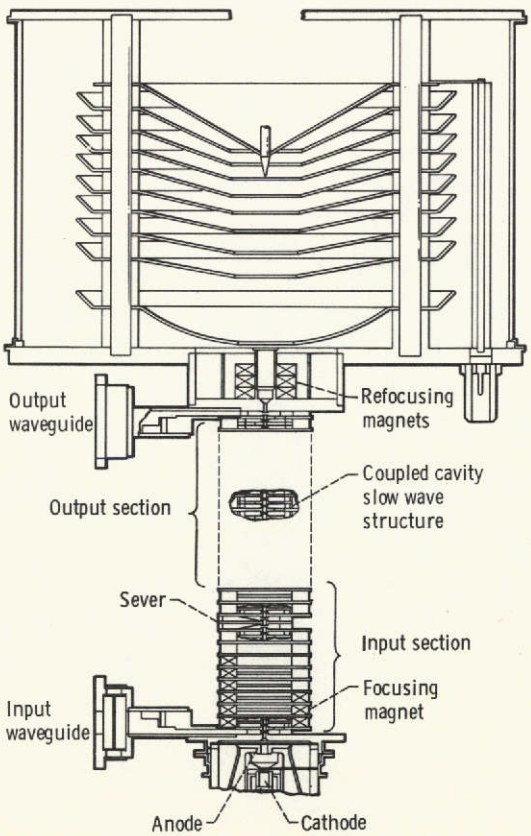

(b) Cross section of coupled cavity traveling wave tube with multistage depressed collector.

Figure 1. - Space communication tube.

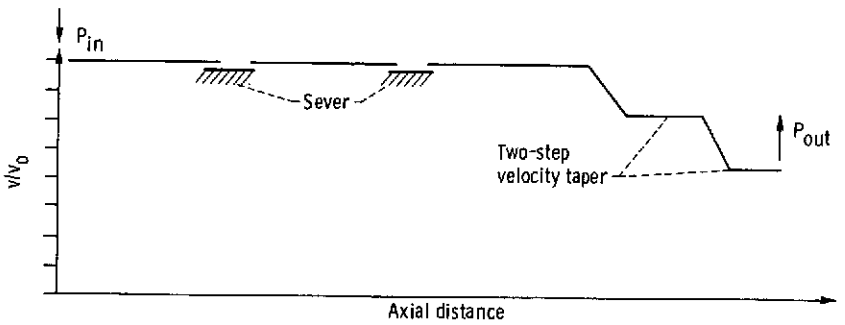

f_0 = 12.06 GHz	$\frac{K_T}{K_0} \approx \left(\frac{v_T}{v_0}\right)^2$	C = 0.056
V_0 = 11 kV		QC = 0.08
I_0 = 61 mA		b = 0
K_0 = 125 Ω	$\frac{L_T}{L_0} \approx \frac{K_0}{K_T}$	d = 0.04
Loss: 0.07 dB/cavity		γa = 0.80

Figure 2. - Velocity profile of 200-watt tube circuit and tube parameters.

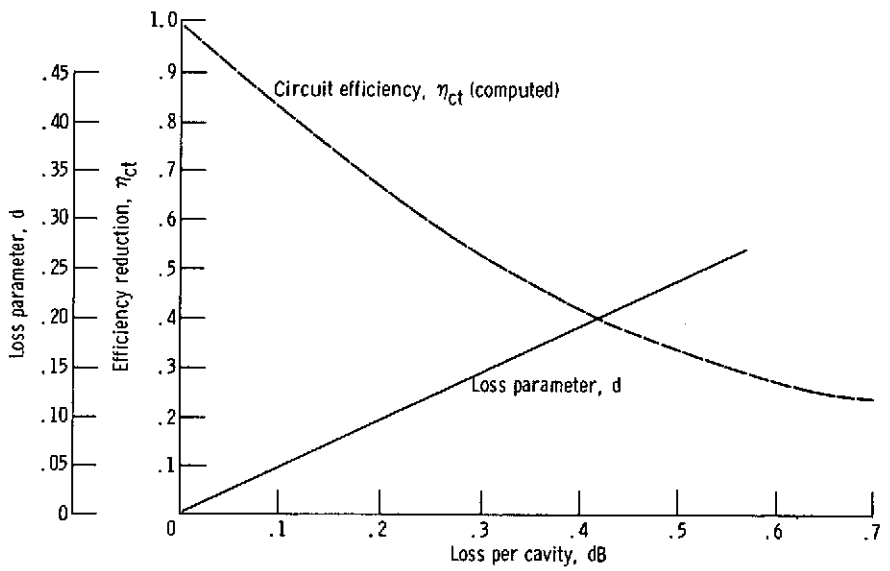

Figure 3. - Predicted efficiency reduction with circuit loss.

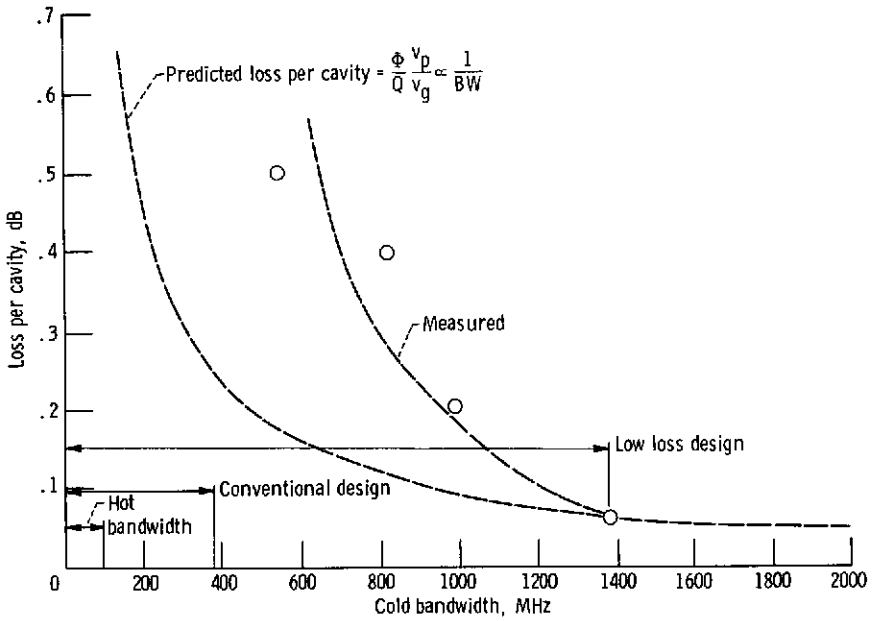

Figure 4. - Effect of cold bandwidth on circuit losses.

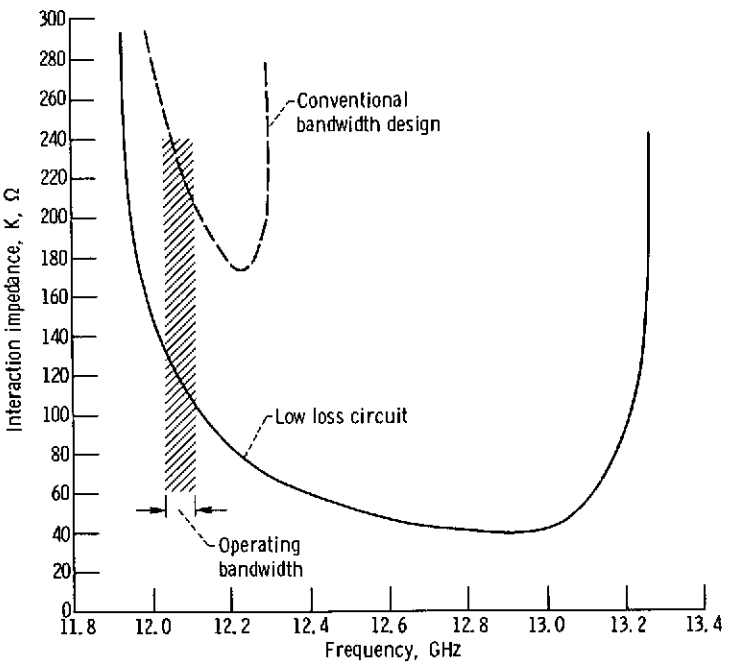

Figure 5. - Interaction impedance for coupled cavity circuits (measured)

$K = \frac{R_s}{Q}\frac{1}{\Phi}\frac{v_p}{v_g} \propto \frac{1}{BW}$.

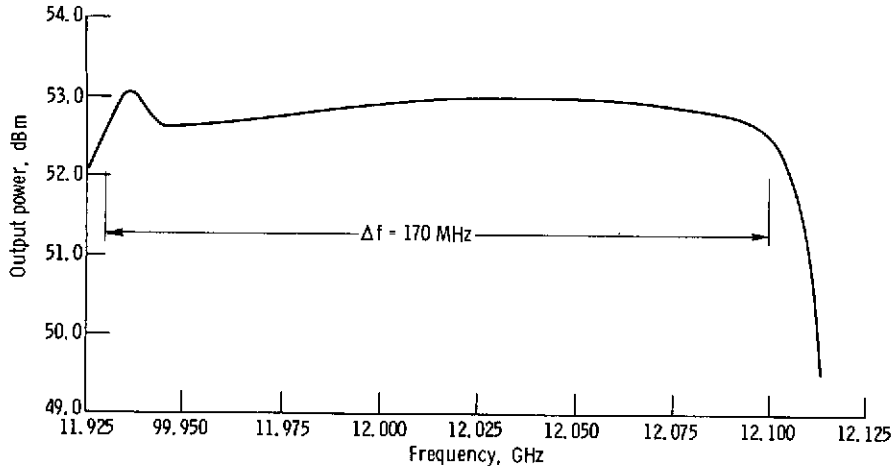

Figure 6. - Bandwidth characteristics with constant drive levels (measured). Cathode to body voltage, V_0, 11.3 kilovolts; dc cathode current, I_0, 64 milliamperes; input power, P_{in}, 16.7 dBm.

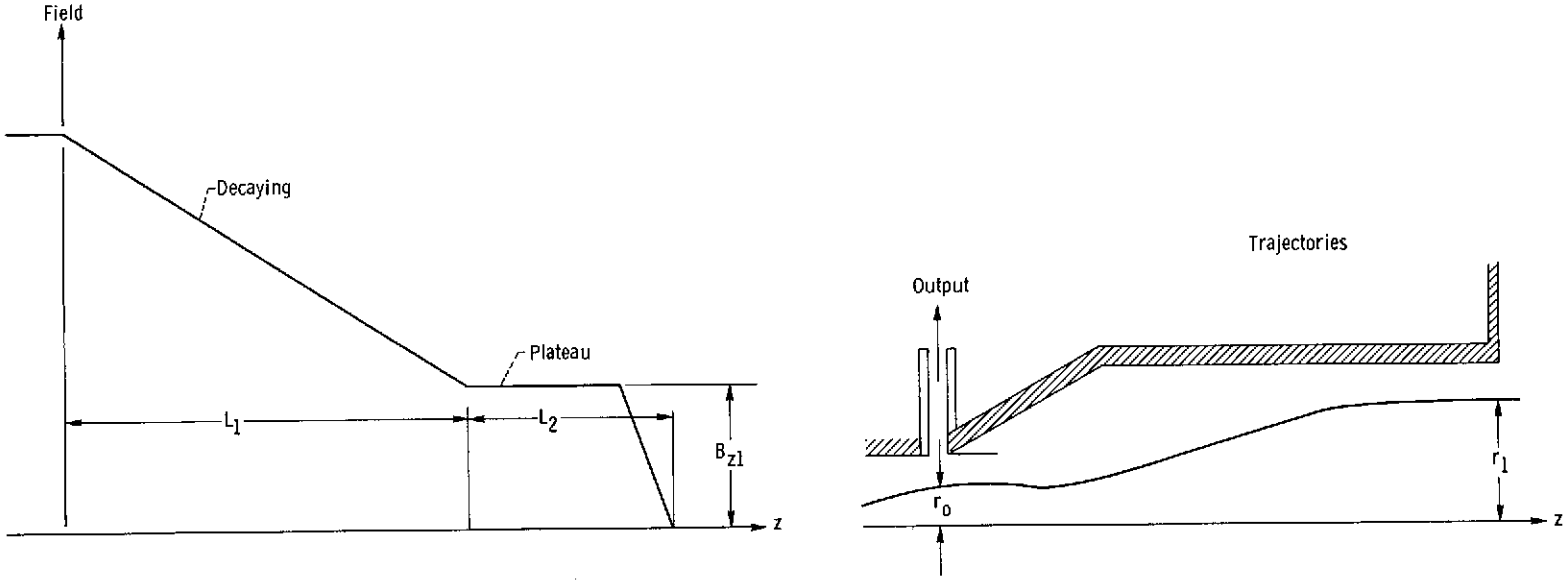

Figure 7. - Schematic of refocusing system.

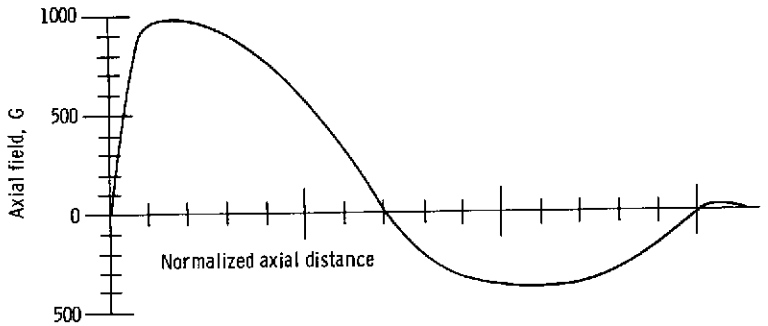

Figure 8. - Refocusing field (measured).

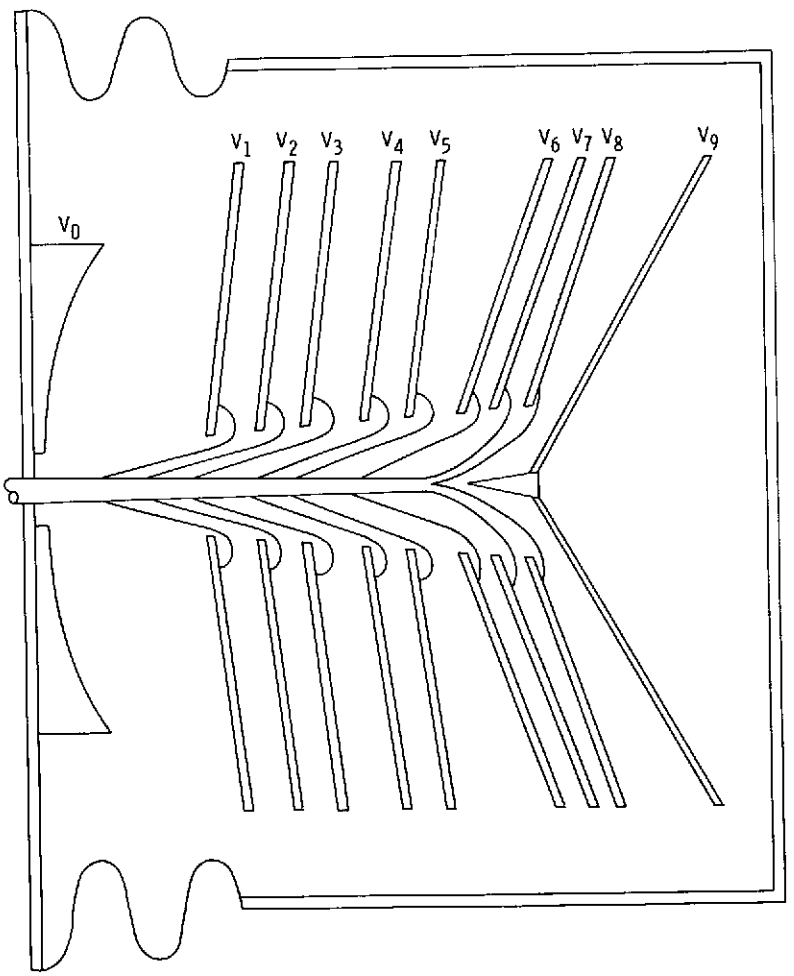

Figure 9. - Schematic of multistage collector.

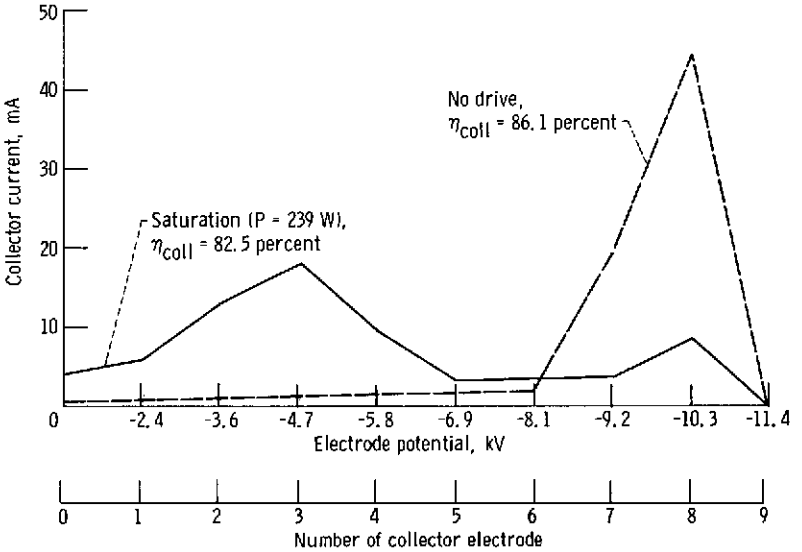

Figure 10. - Collector current distribution (measured). Collector efficiency, $\eta_{coll} = \frac{\text{recovered kinetic beam energy}}{\text{kinetic beam energy into collector}}$. Cathode to body voltage, V_0, 11.3 kilovolts; dc cathode current, I_0, 67 milliamperes.